Published for SISSA by Springer

Received: May 7, 2024
Accepted: July 12, 2024
Published: July 30, 2024

Two-loop mixed QCD-EW corrections to charged current Drell-Yan

Tommaso Armadillo[a,b], **Roberto Bonciani**[c], **Simone Devoto**[b,d], **Narayan Rana**[e] and **Alessandro Vicini**[b,f]

[a] *Centre for Cosmology, Particle Physics and Phenomenology (CP3), Université catholique de Louvain, Chemin du Cyclotron, 2, B-1348 Louvain-la-Neuve, Belgium*

[b] *Dipartimento di Fisica "Aldo Pontremoli", University of Milano and INFN, Sezione di Milano, I-20133 Milano, Italy*

[c] *Dipartimento di Fisica, Università di Roma "La Sapienza" and INFN, Sezione di Roma, I-00185 Roma, Italy*

[d] *Department of Physics and Astronomy, Ghent University, 9000 Ghent, Belgium*

[e] *School of Physical Sciences, National Institute of Science Education and Research, An OCC of Homi Bhabha National Institute, 752050 Jatni, India*

[f] *CERN, Theoretical Physics Department, CH-1211 Geneva 23, Switzerland*

E-mail: tommaso.armadillo@uclouvain.be, roberto.bonciani@roma1.infn.it, simone.devoto@ugent.be, narayan.rana@niser.ac.in, alessandro.vicini@mi.infn.it

Abstract: We present the two-loop mixed strong-electroweak virtual corrections to the charged current Drell-Yan process. The final-state collinear singularities are regularised by the lepton mass. The evaluation of all the relevant Feynman integrals, including those with up to two different internal massive lines, has been worked out relying on semi-analytical techniques, using complex-valued masses. We can provide, at any arbitrary phase-space point, the solution as a power series in the W-boson mass, around a reference value. Starting from these expansions, we can prepare a numerical grid for any value of the W-boson mass within their radius of convergence in a negligible amount of time.

Keywords: Electroweak Precision Physics, Higher Order Electroweak Calculations, Higher-Order Perturbative Calculations

ArXiv ePrint: 2405.00612

https://doi.org/10.1007/JHEP07(2024)265

JHEP07(2024)265

Contents

1 Introduction

The hadro-production of lepton-antilepton or lepton-antineutrino pairs, known, respectively, as neutral current (NC) and charged current (CC) Drell-Yan (DY) processes [1], are crucial at hadron colliders since they provide the environment for a precise study of the gauge sector of the Standard Model (SM) of fundamental interactions. In particular, the NC DY is important for the determination of the Z-boson mass and the effective weak mixing angle, and the CC DY is important for the determination of the W-boson mass. These three electroweak (EW) parameters are known at the moment with small relative errors, 0.01% for the boson masses and 0.1% for the effective weak mixing angle [2–6], originating from a fitting procedure between measured kinematical distributions and generated theoretical templates [7–11].

Due to highly precise experimental data, the control on the precision of these parameters forces the theoretical predictions to involve higher-order perturbative corrections. Next-to-leading-order (NLO) [12] and next-to-next-to-leading-order (NNLO) [13, 14] QCD corrections to the total production cross section of a Z or W boson have been computed more than 30 years ago. The inclusion of the following order in the strong coupling constant α_s, the next-to-next-to-next-to-leading-order (N^{3}LO), has been recently completed for the inclusive production of a virtual photon [15], a W [16], and a Z boson [17]. The NNLO QCD corrections

JHEP07(2024)265

have been implemented at the fully differential level in [18–22]. Fiducial cross sections for the NC DY and CC DY processes at N^{3}LO QCD have been computed in [23–26]. Finally, more exclusive observables, as the di-lepton rapidity distribution and the transverse mass and charge asymmetry, have been computed to third order in QCD in [27] and [28], respectively. The resummation of logharithmically enhanced terms near the production threshold has been considered in [29–37]. NLO EW corrections are known both for W [38–42], and for Z production [43–47].

The combination of NLO QCD and EW results with QCD and QED Parton Showers, has been presented in [48–52]. At the required level of accuracy, NNLO mixed QCD×EW corrections are also relevant in particular for kinematical distributions [7].

For on-shell inclusive Z production, the NNLO QCD×QED corrections have been calculated in [53]. Exclusive on-shell Z-boson production has been considered in [54] and in [55]. The complete NNLO mixed QCD×EW corrections to the total cross section of production of an on-shell Z boson have been presented in [56–59], while in [60] and [61] the same corrections have been evaluated differentially in the final-state leptonic variables for on-shell Z and W production respectively.

Mixed QCD×EW corrections at the W or Z resonances has been evaluated in pole approximation in [62, 63]. In [64] the gauge-invariant set of corrections that include a closed fermionic loop, at $\mathcal{O}(n_F\alpha_s\alpha)$, with α the fine-structure constant and n_F the number of active flavors, were evaluated for off-shell Z and W production. In the case of NC DY, recently, differential distributions and the forward-backward asymmetry have been evaluated in pole approximation in [65].

The complete set of NNLO QCD×EW corrections to the NC DY process $pp \to \ell^+\ell^- + X$ is available and has been presented in [66], for massive leptons, and in [67] for massless leptons. The calculation in [66] is based on the exact two-loop amplitudes presented in [68], evaluated through the reduction to the master integrals [69] and a semi-analytical implementation of the differential equations method for their calculation [70–72]. The IR singularities have been treated in the q_{T} subtraction formalism [73, 74], implemented in the MATRIX framework [75]. The calculation in [67] is based on the exact amplitudes presented in [76] expressed in terms of master integrals evaluated in analytic polylogarithmic form [77, 78].

For the CC DY process $pp \to \ell\nu_\ell + X$, the mixed QCD×EW corrections have been computed in [79], in the case of massive lepton, with approximated two-loop virtual corrections. While the full set of double-real and real-virtual contributions due to initial and final state radiation have been included in the analysis in exact form, the finite part of the two-loop virtual amplitudes has been evaluated in pole approximation. Large mixed QCD×EW effects might develop in the large lepton-pair transverse/invariant mass limit, where the pole approximation is expected to become less accurate, and are relevant for new physics searches. In this paper, we calculate the virtual two-loop amplitude at $\mathcal{O}(\alpha_s\alpha)$ exactly. Final-state collinear divergences are regularized by the finite mass of the final-state lepton. We keep the exact dependence on the masses of the vector bosons and we find expressions that are valid in the whole physical phase-space. In section 2, we provide the framework of our computation, with the description of the ultraviolet (UV) renormalisation procedure. In section 3, the details of the computation are presented, from the amplitude level up to the renormalised

JHEP07(2024)265

matrix elements. In section 4, the infrared (IR) subtraction procedure is discussed and we describe how we obtain the UV renormalised IR subtracted finite remainder. In section 5 we present our numerical results. Finally, in section 6 we draw our conclusions. The unrenormalised matrix elements in terms of master integrals are provided as supplementary material. Appendix A gives the reader the information needed to make use of the files.

2 Framework of the calculation

2.1 The process

The process under study is the production of a lepton-neutrino pair in quark-antiquark annihilation

$$u(p_1) + \bar{d}(p_2) \to \nu_\ell(p_3) + \ell^+(p_4)\,. \tag{2.1}$$

We consider the two-loop mixed QCD-EW corrections to this reaction,[1] with explicit results for massless initial-state quarks. This partonic process has a bare amplitude,[2] which admits a perturbative expansion in the two coupling constants

$$|\hat{\mathcal{M}}\rangle = |\hat{\mathcal{M}}^{(0)}\rangle + \left(\frac{\hat{\alpha}_s}{4\pi}\right)|\hat{\mathcal{M}}^{(1,0)}\rangle + \left(\frac{\hat{\alpha}}{4\pi}\right)|\hat{\mathcal{M}}^{(0,1)}\rangle + \left(\frac{\hat{\alpha}_s}{4\pi}\right)\left(\frac{\hat{\alpha}}{4\pi}\right)|\hat{\mathcal{M}}^{(1,1)}\rangle + \cdots \tag{2.2}$$

We compute the interference terms:[3]

$$\langle\hat{\mathcal{M}}^{(0)}|\hat{\mathcal{M}}^{(1,0)}\rangle\,, \quad \langle\hat{\mathcal{M}}^{(0)}|\hat{\mathcal{M}}^{(0,1)}\rangle\,, \quad \langle\hat{\mathcal{M}}^{(0)}|\hat{\mathcal{M}}^{(1,1)}\rangle\,, \tag{2.3}$$

which contribute to the unpolarised squared matrix element of the process in eq. (2.1), at $\mathcal{O}(\alpha\alpha_s)$. The virtual corrections to any scattering process amplitude are in general affected by singularities of UV and IR type, which we regularise working in $d = 4 - 2\varepsilon$ space-time dimensions. We apply the integration-by-parts (IBP) [80, 81] and Lorentz invariance (LI) [82] identities to reduce all the scalar Feynman integrals appearing in the interference terms (2.3) to a limited set, the so-called Master Integrals (MIs). The final expression can then be cast as the sum of the MIs multiplied by their associated coefficients. The latter depend, as rational functions, on the kinematical invariants of the process, the masses of the internal particles exchanged in the Feynman diagrams, and the dimensional regularization parameter ε.

The d-dimensional nature of an EW computation performed in dimensional regularisation requires the extension to d dimensions of the inherently 4-dimensional object γ_5. In this work we follow the same strategy outlined in [68], preserving the anti-commutation proprieties of γ_5 in a fixed-point prescription. We refer the reader to [68] for more details on the procedure.

The cancellation of the UV divergences follows according to a standard renormalisation procedure. The resulting amplitudes are expressed in terms of renormalised parameters, in turn related to measurable quantities. The IR divergences have a universal structure, arising

[1] The production of the $\ell^-\bar{\nu}_\ell$ final state can be obtained with a fully analogous calculation, or, assuming CP invariance, from the amplitude for the positively charged final state, with appropriate transformations of the external momenta.

[2] We denote by *hat* the bare quantities.

[3] We do not discuss the interference term $\langle\hat{\mathcal{M}}^{(0,1)}|\hat{\mathcal{M}}^{(1,0)}\rangle$, also contributing at $\mathcal{O}(\alpha\alpha_s)$, which can be easily obtained with any NLO amplitude generator.

JHEP07(2024)265

from the behavior of the amplitudes in the soft and/or collinear limit. The universality of the divergent factors has been discussed at length in the literature and allows us to prepare a subtraction term, which is independent of the details of the full two-loop calculation, and depends only on the lower order amplitudes. We exploit the universality property to check the consistency of our computation, for the prescription related to the Dirac γ_5 matrix. We write the UV-renormalised amplitude as a Laurent expansion in ε. We have, at one- and two-loop level respectively:

$$\langle \mathcal{M}^{(0)} | \mathcal{M}^{(0,1)} \rangle = \sum_{i=-2}^{2} \varepsilon^i C_i^{(0,1)}(s,t,\mu_W,\mu_Z,m_\ell)\,, \tag{2.4}$$

$$\langle \mathcal{M}^{(0)} | \mathcal{M}^{(1,0)} \rangle = \sum_{i=-2}^{2} \varepsilon^i C_i^{(1,0)}(s,t,\mu_W,\mu_Z,m_\ell)\,, \tag{2.5}$$

and

$$\langle \mathcal{M}^{(0)} | \mathcal{M}^{(1,1)} \rangle = \sum_{i=-4}^{0} \varepsilon^i C_i^{(1,1)}(s,t,\mu_W,\mu_Z,m_\ell)\,. \tag{2.6}$$

In eq. (2.6) only terms up to ε^0 have been kept, because we are interested in the finite contributions at NNLO only. The higher powers of ε would be relevant for higher-order calculations. The lepton mass is labelled by m_l. Given the mass and decay width M_V, Γ_V of the gauge boson V ($V = W, Z$), we define μ_V as the position in the complex plane of the pole of the boson propagator

$$\mu_V^2 = M_V^2 - i M_V \Gamma_V\,. \tag{2.7}$$

The Mandelstam variables are defined as:

$$s = (p_1+p_2)^2,\ t = (p_1-p_3)^2,\ u = (p_2-p_3)^2 \text{ with } s+t+u = m_l^2\,, \tag{2.8}$$

while the on-shell conditions of the external particles are:

$$p_1^2 = p_2^2 = p_3^2 = 0;\ p_4^2 = m_l^2; \tag{2.9}$$

The main result of this paper is the IR-subtracted expressions that can be obtained by the combination of the two-loop coefficients $C_i^{(1,1)}$ in eq. (2.6) with the universal subtraction term. The latter is based on the availability of the Born and the one-loop matrix elements in eqs. (2.4), (2.5).

2.2 Ultraviolet renormalisation

The NC DY process renormalisation, at $\mathcal{O}(\alpha\alpha_s)$, has already been discussed in detail in [64, 68]. For the CC DY process we follow similar steps, that we summarize in this section.

2.2.1 Charge renormalisation

The $\mathrm{SU}(2)_L$ and $\mathrm{U}(1)_Y$ bare gauge couplings g_0, g_0' and the Higgs doublet vacuum expectation value v_0 can be related, with appropriate counterterms, to their renormalised counterparts g, g', v. We link g, g', v to a set of three measurable quantities: for instance G_μ, μ_W, μ_Z (which

JHEP07(2024)265

we dub G_μ-scheme, with G_μ the Fermi constant) or e, μ_W, μ_Z (which we dub α-scheme, with $\alpha = e^2/(4\pi)$ the fine structure constant and e the positron charge). The choice of the three measurable quantities defines the so called input scheme. The relation between bare and renormalised input parameters is

$$\mu_{W0}^2 = \mu_W^2 + \delta\mu_W^2, \quad \mu_{Z0}^2 = \mu_Z^2 + \delta\mu_Z^2, \quad e_0 = e + \delta e\,. \tag{2.10}$$

The on-shell electric charge counterterm δe at $\mathcal{O}(\alpha^2)$ and $\mathcal{O}(\alpha\alpha_s)$ has been discussed in [83], from the study of the Thomson scattering. The mass counterterms $\delta\mu_W^2$, $\delta\mu_Z^2$ in the complex mass scheme [84] have been presented in [64]. In terms of the transverse part of the unrenormalised VV gauge boson self-energies, which are defined in [85], they are:

$$\delta\mu_V^2 = \Sigma_T^{VV}(\mu_V^2)\,, \tag{2.11}$$

at the pole in the complex plane $q^2 = \mu_V^2$ of the gauge boson propagator, with $V = W, Z$. From the study of the muon-decay amplitude, we derive the following relation

$$\frac{G_\mu}{\sqrt{2}} = \frac{\pi\alpha}{2}\frac{\mu_Z^2}{\mu_W^2(\mu_Z^2 - \mu_W^2)}\,(1 + \Delta r)\ . \tag{2.12}$$

The finite correction Δr has been introduced, with real gauge boson masses, in [86] and its $\mathcal{O}(\alpha\alpha_s)$ corrections were presented in [87, 88]. We evaluate it here with complex-valued masses.

We consider now the bare couplings which appear at tree-level in the interaction of the photon and W boson with fermions. The UV divergent correction factors $\delta g_W^{G_\mu}$ and δg_W^{α} contribute to the charge renormalisation of the $Wf\bar{f}'$ vertex in the G_μ- and α-scheme, respectively, as

$$g_0 = \sqrt{4\sqrt{2}G_\mu\mu_W^2}\left[1 - \frac{1}{2}\Delta r + \frac{\delta e}{e} + \frac{1}{2}\frac{\mu_W^2}{\mu_Z^2 - \mu_W^2}\left(\frac{\delta\mu_W^2}{\mu_W^2} - \frac{\delta\mu_Z^2}{\mu_Z^2}\right)\right] \tag{2.13}$$

$$\equiv \sqrt{4\sqrt{2}G_\mu\mu_W^2}\left(1 + \delta g_W^{G_\mu}\right) \tag{2.14}$$

and

$$g_0 = e\sqrt{\frac{\mu_Z^2}{\mu_Z^2 - \mu_W^2}}\left[1 + \frac{\delta e}{e} + \frac{1}{2}\frac{\mu_W^2}{\mu_Z^2 - \mu_W^2}\left(\frac{\delta\mu_W^2}{\mu_W^2} - \frac{\delta\mu_Z^2}{\mu_Z^2}\right)\right] \tag{2.15}$$

$$\equiv e\sqrt{\frac{\mu_Z^2}{\mu_Z^2 - \mu_W^2}}\left(1 + \delta g_W^{G_\alpha}\right)\ . \tag{2.16}$$

Working out the explicit expression of $\delta g_Z^{G_\mu}$, the dependence on the electric charge counterterm cancels out.

The counterterm contributions to the renormalised amplitude are obtained by replacing the bare couplings in the lower order amplitudes with the expressions presented in eqs. (2.14)–(2.16) and expanding δg_W up to the relevant perturbative order. We show in the next section how δg_W enters in the renormalisation of the W boson propagators.

JHEP07(2024)265

2.2.2 Renormalisation of the gauge boson propagators

The renormalised gauge boson self-energies are obtained, at $\mathcal{O}(\alpha)$, by combining the unrenormalised self-energy expressions with the mass and wave function counterterms. In the full calculation, which includes the quark doublets of the three fermion families, we never introduce wave function counterterms on the internal lines, because they would systematically cancel against a corresponding factor stemming from the definition of the renormalised vertices. We exploit instead the relation in the SM between the wave function and charge counterterms [85] and we directly use the latter to define the renormalised self-energies. We obtain:

$$\Sigma_{R,T}^{WW}(q^2) = \Sigma_T^{WW}(q^2) - \delta\mu_W^2 + 2\,(q^2 - \mu_W^2)\,\delta g_W\,, \tag{2.17}$$

where $\Sigma_{R,T}^{VV}$ is the transverse part of the renormalised VV vector boson self-energy. The charge counterterms have been defined in eqs. (2.14)–(2.16). At $\mathcal{O}(\alpha\alpha_s)$ the structure of these contributions does not change: the corrections to the gauge boson self-energies stem from a quark loop with one internal gluon exchange and, in addition, from the $\mathcal{O}(\alpha_s)$ mass renormalisation of the quark lines in the one-loop self-energies.

The expression of the two-loop Feynman integrals required for the evaluation of the $\mathcal{O}(\alpha\alpha_s)$ correction to the gauge boson propagators and all the needed counterterms can be found in [64, 87, 88].

3 The UV-renormalised unsubtracted amplitude

3.1 Generation of the full amplitude and evaluation of the interference terms

Different kinds of Feynman diagrams contribute, at $\mathcal{O}(\alpha\alpha_s)$, to the scattering amplitude, and we compute them using the background field gauge (BFG) [89]. We present[4] in figures 1 and 2 a few representative examples. The initial state two-loop vertex corrections (figure 1-(a)), are combined with the two-loop external quark wave function corrections (figure 1-(b)) and with the one-loop external quark wave function correction with initial-state QCD vertex correction (figure 2-(f)). The combination yields an UV-finite, but still IR-divergent, result. We treat as a separate subset the sum of two-loop W self-energy, together with the corresponding two-loop mass counterterms and with the insertion of charge renormalisation constants in the initial and final state vertices. Representative diagrams are shown in figures 1-(c),(d),(e). The combination yields an UV- and IR-finite contribution. An example of a two-loop box with the exchange of one W and one neutral EW boson is given in figure 1-(f). We remark the absence of contributions from closed fermionic triangles, because of colour conservation.

The factorisable contributions are schematically represented in figures 2-(a),(f). They all include, at $\mathcal{O}(\alpha\alpha_s)$, an initial-state QCD vertex correction. The second factor can be, alternatively: the final-state EW vertex corrections, the external lepton wave function correction, the one-loop W self-energy corrections, the one-loop W mass renormalisation counterterms, the one-loop external quark wave function correction and the one-loop charge renormalisation contributions. The properties of the BFG allow to identify UV-finite Feynman diagrams combinations.

[4]The straight line with an arrow represents a fermion line (blue: quark, red: leptons), the wavy lines represent EW gauge bosons (green: W, red: Z, black: photon) and the spiral coils represent gluons.

JHEP07(2024)265

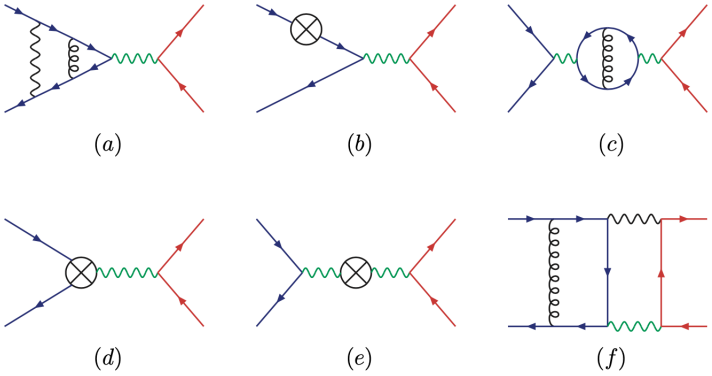

Figure 1. Sample Feynman diagrams of two-loop corrections and associated two-loop counterterms.

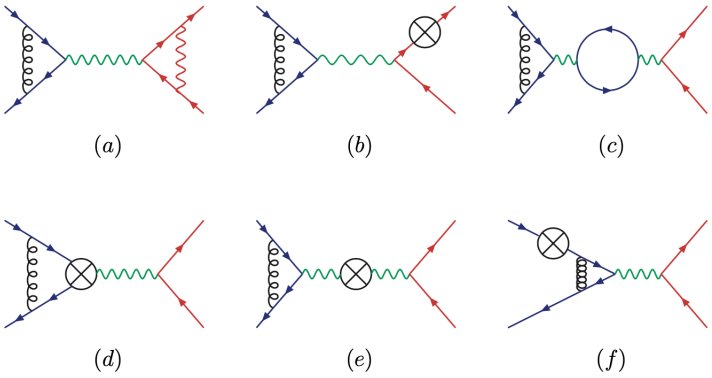

Figure 2. Sample Feynman diagrams of factorisable corrections, including one-loop counterterm corrections.

We follow a general procedure to compute the bare matrix elements up to two-loop order. We generate the Feynman diagrams with two completely independent approaches, one based on FeynArts [90] and a second one on QGRAF [91]. The in-house Mathematica package ABISS has been used to perform the Lorentz and Dirac algebra and obtain the interference between the virtual corrections and the Born amplitude. It has been compared with the independent results of a second set of procedures written in FORM [92]. The large number of scalar Feynman integrals appearing in the intermediate expressions is reduced to a smaller set of MIs by means of IBP and LI identities. The reduction algorithms are implemented in two independent in-house programs based on Kira [93] and LiteRed [94, 95]. We have cross-checked at one- and two-loop level the corresponding expressions, finding perfect agreement. Additional technical details, common to the NC and CC DY processes, are described in [68].

We retain the exact dependence on the lepton mass m_ℓ, both at the one- and two-loop level, only in the diagrams where an internal photon couples to the final-state lepton, featuring the complete set of contributions enhanced by $\log(m_\ell^2)$. The lepton mass regulates in this case the final-state collinear divergences. These diagrams also yield a gauge-invariant subset of terms proportional to m_ℓ^2/μ_W^2, which are however phenomenologically negligible. In all the other cases, we do not have final-state IR divergences, and therefore we can keep the lepton

JHEP07(2024)265

massless. The use of this approximation reduces by one the number of independent mass scales in the computation and thus its complexity, allowing for a faster evaluation of the amplitude.

3.2 Integral families and the representation of the result in terms of MIs

The scattering amplitude, after the computation of the interference terms, appears as a sum of scalar Feynman integrals.

In order to classify all the integrals entering in our computation, we need 11 different integral families. Among them, 7 can be defined exactly as the ones introduced in [68] for the case of the NC DY process:

$$\begin{aligned}
\mathrm{B}_0 &: \{\mathcal{D}_1, \mathcal{D}_2, \mathcal{D}_{12}, \mathcal{D}_{1;1}, \mathcal{D}_{2;1}, \mathcal{D}_{1;12}, \mathcal{D}_{2;12}, \mathcal{D}_{1;3}, \mathcal{D}_{2;3}\} \\
\mathrm{B}_1 &: \{\mathcal{D}_1, \mathcal{D}_2, \mathcal{D}_{12}, \mathcal{D}_{1;1}, \mathcal{D}_{2;1}, \mathcal{D}_{1;12}, \mathcal{D}_{12;2}, \mathcal{D}_{1;3}, \mathcal{D}_{2;3}\} \\
\mathrm{B}_{11} &: \{\mathcal{D}_1, \mathcal{D}_2, \mathcal{D}_{12} - \mu_V^2, \mathcal{D}_{1;1}, \mathcal{D}_{2;1}, \mathcal{D}_{1;12}, \mathcal{D}_{2;12}, \mathcal{D}_{1;3}, \mathcal{D}_{2;3}\} \\
\mathrm{B}_{12} &: \{\mathcal{D}_1, \mathcal{D}_2, \mathcal{D}_{12}, \mathcal{D}_{1;1} - \mu_V^2, \mathcal{D}_{2;1}, \mathcal{D}_{1;12}, \mathcal{D}_{2;12}, \mathcal{D}_{1;3}, \mathcal{D}_{2;3}\} \\
\mathrm{B}_{13} &: \{\mathcal{D}_1, \mathcal{D}_2, \mathcal{D}_{12} - \mu_V^2, \mathcal{D}_{1;1}, \mathcal{D}_{2;1}, \mathcal{D}_{1;12}, \mathcal{D}_{12;2}, \mathcal{D}_{1;3}, \mathcal{D}_{2;3}\} \\
\mathrm{B}_{14} &: \{\mathcal{D}_1, \mathcal{D}_2 - \mu_V^2, \mathcal{D}_{12}, \mathcal{D}_{1;1}, \mathcal{D}_{2;1}, \mathcal{D}_{1;12}, \mathcal{D}_{2;12}, \mathcal{D}_{1;3}, \mathcal{D}_{2;3}\} \\
\mathrm{B}_{18} &: \{\mathcal{D}_1, \mathcal{D}_2, \mathcal{D}_{12}, \mathcal{D}_{1;1}, \mathcal{D}_{2;1}, \mathcal{D}_{1;12}, \mathcal{D}_{2;12}, \mathcal{D}_{1;3} - \mu_V^2, \mathcal{D}_{2;3} - \mu_V^2\}\,,
\end{aligned} \tag{3.1}$$

where V can be either Z or W, and we have defined the denominators $\mathcal{D}$ as follows:

$$\mathcal{D}_i = k_i^2, \mathcal{D}_{ij} = (k_i - k_j)^2, \mathcal{D}_{i;j} = (k_i - p_j)^2, \mathcal{D}_{i;jl} = (k_i - p_j - p_l)^2, \mathcal{D}_{ij;l} = (k_i - k_j - p_l)^2 \tag{3.2}$$

The remaining 4 integral families only appear for the case of CC DY:

$$\begin{aligned}
\tilde{\mathrm{B}}_{14} &: \{\mathcal{D}_1, \mathcal{D}_2 - \mu_V^2, \mathcal{D}_{12}, \mathcal{D}_{1;1}, \mathcal{D}_{2;1}, \mathcal{D}_{1;12}, \mathcal{D}_{2;12}, \mathcal{D}_{1;3}, \mathcal{D}_{2;3} - m_\ell^2\} \\
\tilde{\mathrm{B}}_{14p} &: \{\mathcal{D}_1, \mathcal{D}_2 - \mu_V^2, \mathcal{D}_{12}, \mathcal{D}_{1;2}, \mathcal{D}_{2;2}, \mathcal{D}_{1;12}, \mathcal{D}_{2;12}, \mathcal{D}_{1;3}, \mathcal{D}_{2;3} - m_\ell^2\} \\
\tilde{\mathrm{B}}_{16} &: \{\mathcal{D}_1, \mathcal{D}_2 - \mu_{V_1}^2, \mathcal{D}_{12}, \mathcal{D}_{1;1}, \mathcal{D}_{2;1}, \mathcal{D}_{1;12}, \mathcal{D}_{2;12} - \mu_{V_2}^2, \mathcal{D}_{1;3}, \mathcal{D}_{2;3}\} \\
\tilde{\mathrm{B}}_{16p} &: \{\mathcal{D}_1, \mathcal{D}_2 - \mu_{V_1}^2, \mathcal{D}_{12}, \mathcal{D}_{1;2}, \mathcal{D}_{2;2}, \mathcal{D}_{1;12}, \mathcal{D}_{2;12} - \mu_{V_2}^2, \mathcal{D}_{1;3}, \mathcal{D}_{2;3}\}\,,
\end{aligned} \tag{3.3}$$

where V_1 and V_2 are two different vector bosons.

The integral families listed in eq. (3.3), despite being specific to the charged current case, can also be seen as an extension of integral families already appearing in the neutral current process, where the value of the masses in the propagators has been modified. In particular, $\tilde{\mathrm{B}}_{16}$ describes box integrals with a W-Z exchange and is the natural extension of B_{16}, already introduced in [68] to describe the Z-Z and W-W box integrals. The latter can in fact be obtained from $\tilde{\mathrm{B}}_{16}$ in the equal mass limit $\mu_{V_1} \to \mu_V$, $\mu_{V_2} \to \mu_V$. Similarly, by considering a massless lepton, $m_\ell = 0$, in the integral family $\tilde{\mathrm{B}}_{14}$, we retrieve the integral family B_{14} listed in eq. (3.1).

In the NC DY case, we introduced the integral family B_{14} instead of the more general $\tilde{\mathrm{B}}_{14}$ because the final state collinear singularities, like e.g. those stemming from the γ-Z boxes, were cancelling between different contributions [96]. We were thus able to take the massless limit for this subset of diagrams. The integral family B_{14} yields collinear poles in dimensional regularization, while such singularities appear in $\tilde{\mathrm{B}}_{14}$ as lepton-mass logarithms.

JHEP07(2024)265

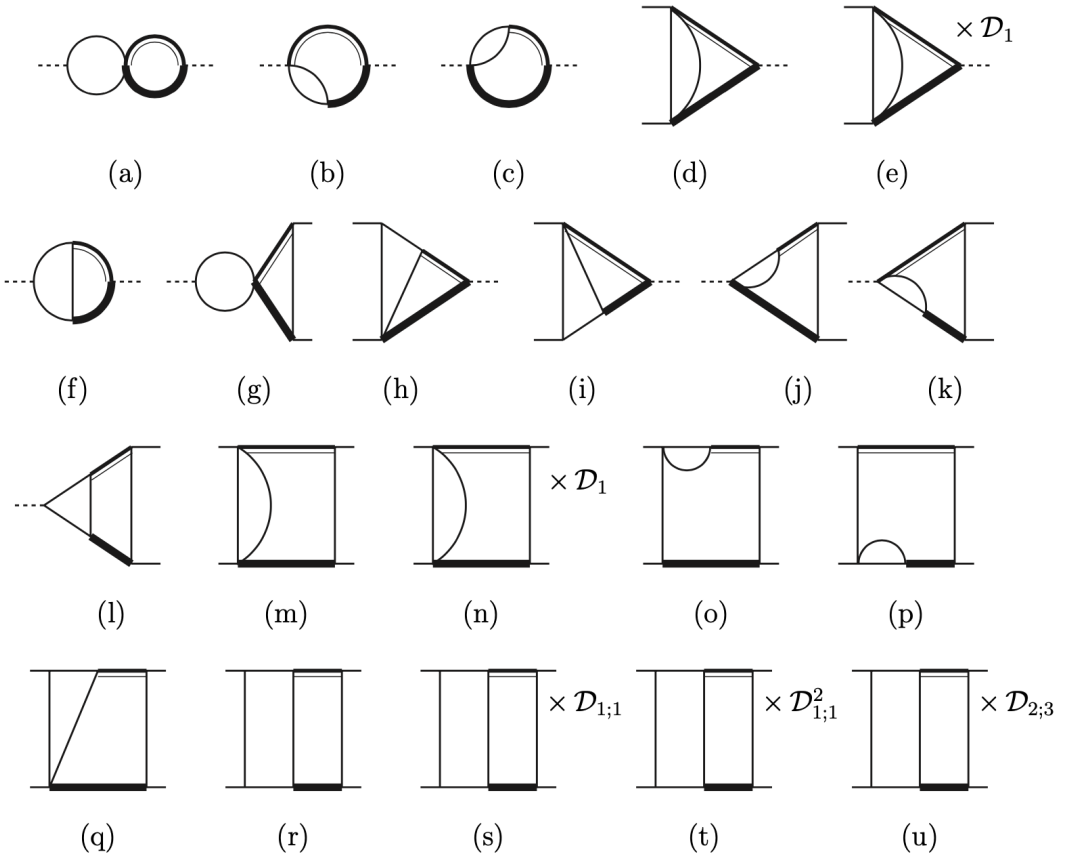

Figure 3. Master Integrals with two different internal masses, belonging to topology $\tilde{B}_{16}$. Thin plane lines represent massless particles. Thick and double lines represent massive particles. External dashed lines indicate the Mandelstam invariant s.

After performing the reduction to MIs, the bare result can be cast in the following, compact form:

$$\langle \hat{\mathcal{M}}^{(0)} | \hat{\mathcal{M}}^{(1,1)} \rangle = \sum_{k=1}^{274} c_k(s,t,\{m_i\},\varepsilon) I_k(s,t,\{m_i\},\varepsilon) \tag{3.4}$$

where c_k are rational coefficients, functions of the kinematical invariants (s,t), the set of real and complex masses $\{m_i\}$ and of the regularisation parameter ε, while I_k are the MIs.[5] In addition to the MIs employed for the NC DY, in the case of the CC DY we have to evaluate two more sets. In figure 3 we show the additional MIs belonging to topology $\tilde{B}_{16}$, that, therefore, have two different masses in the propagators. In figure 4, instead, we show the MIs of topology $\tilde{B}_{14}$, that have two different masses in the propagators and a massive external leg.

3.3 Numerical evaluation of MIs via series expansions

The final step of the calculation consists in the numerical evaluation of the MIs. The additional complication of the charged-current calculation, with respect to the neutral-current

[5]This intermediate result is provided as supplementary material attached to this paper.

JHEP07(2024)265

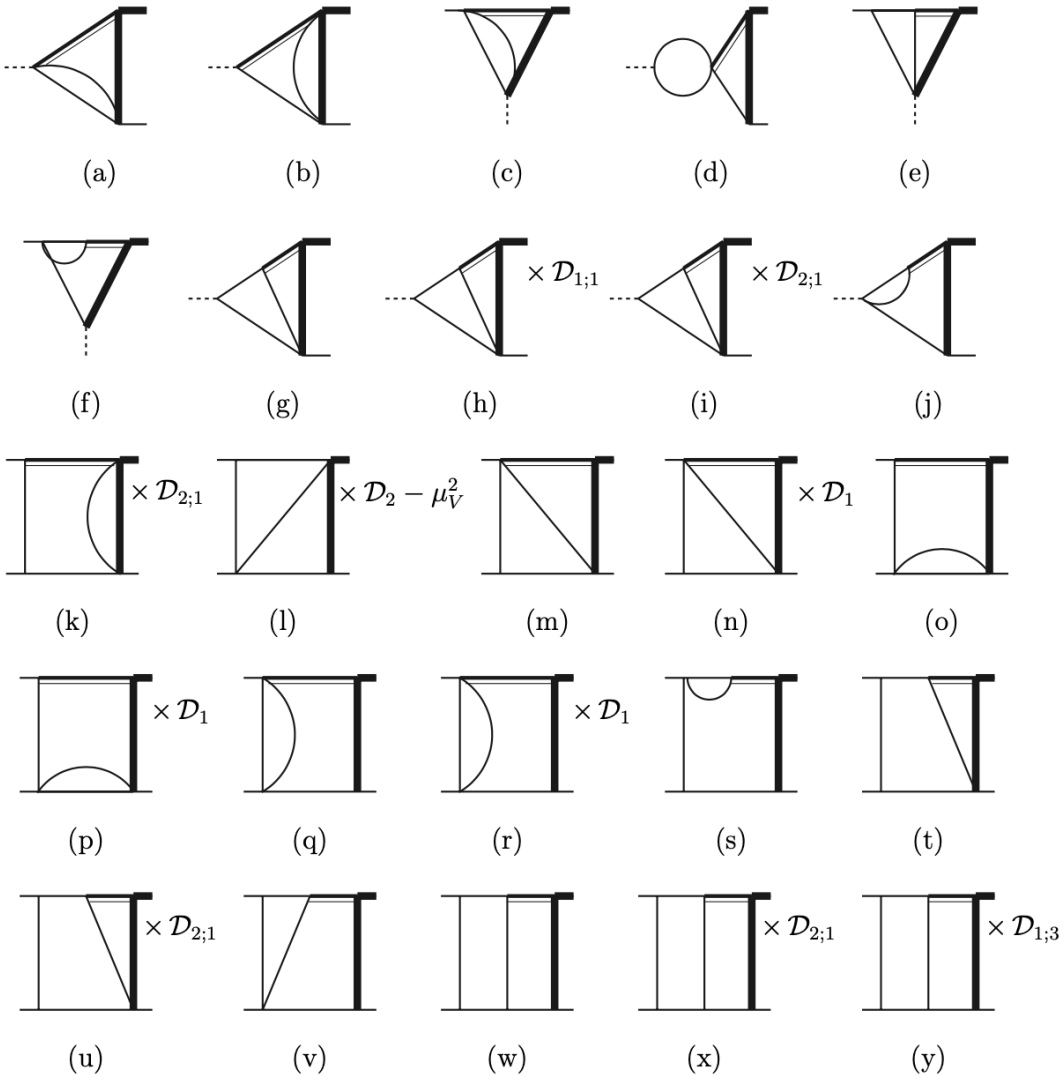

Figure 4. Master Integrals with two different masses, belonging to topology $\tilde{B}_{14}$. Thin plane lines represent massless particles. Thick and double lines represent massive particles. External dashed lines indicate the Mandelstam invariant s.

one presented in [68], is given by the presence of the $\tilde{B}_{14}$ and $\tilde{B}_{16}$ topologies, that are two-loop boxes with two internal (and one external in the case of $\tilde{B}_{14}$), and different, massive lines. In the case of $\tilde{B}_{16}$, the analytical result for the equal masses case has been presented in [69] in terms of Chen-iterated integrals and an analytical expression in terms of GPLs has been found in [77]. However, for the different masses case, no analytical expressions are available in the literature. We have opted to compute the integrals using the series expansion approach.

We have generated the differential equations using in-house MATHEMATICA routines, which rely on the external package LITERED for computing the derivatives with respect to kinematic invariants s and t and on the IBPs relations provided by KIRA. The boundary conditions for all the MIs have been computed in a point in the physical region by using AMFLOW [97], interfaced with KIRA. Their numerical evaluation, up to 50 digits, requires

JHEP07(2024)265

$\sim$ 4.5h on a laptop using 8 threads. Finally, we have solved the system of differential equations in the Mandelstam variables s and t using the MATHEMATICA package SEASYDE [72], that allows us to consider complex-valued internal masses.

Since when combining the numerical values of the MIs with their rational coefficients big numerical cancellations can occur, it is extremely important to keep under control the numerical precision of the evaluation of the MIs. Within SEASYDE, we have decided to keep 70 terms in the expansion in the kinematic invariants. The estimate for the relative error provided by SEASYDE is, at worst, 10^{-14} in every point of the phase-space.[6] In several points of the phase-space we have performed a cross-check against AMFLOW by computing the MIs with 50 digits precision, finding agreement for the first 14 digits, in accordance to the uncertainty estimated by SEASYDE. Cross-checks with analytical expressions, when available, have been performed as-well, finding agreement.

Using SEASYDE we were able to generate a numerical grid in $(\sqrt{s}, \cos\theta)$, consisting in 3250 points, as described in detail in section 5.1. The numerical evaluation of the complete grid for all the topologies requires, in total, $\sim$ 3 weeks on a cluster with 26 cores. The most complicated case is the two-loop box with two massive internal lines, for which we have to solve a system with 56 equations. The calculation of its grid requires $\sim$ 10 days by itself.

3.3.1 Mass evolution

Finally, we have done a self-consistency check by exploiting the flexibility given by the method of differential equations and the series expansion approach. We observe, indeed, that in the limit of the two masses being equal, the $\tilde{B}_{16}$ topology reduces to the B_{16} from the neutral-current case. Hence, another way for computing a numerical grid for $\tilde{B}_{16}$ is, firstly, to create a numerical grid in (s, t) for B_{16} and, secondly, to write down the differential equations w.r.t. one of the two masses to evolve B_{16} to $\tilde{B}_{16}$. We have explicitly verified, for different points in the phase-space, that the result obtained by evolving the equal masses box in s and t and then in one of the two masses, is in agreement with the one obtained by evolving directly the two-masses box in the Mandelstam variables s and t. The two possibilities are schematically depicted in figure 5.

3.4 Additional comments on the numerical evaluation of MIs

In this work, our main objective is to pursue the automation of all the steps in the calculation of virtual corrections, in particular, the numerical evaluation of the MIs. Within our framework, all the steps are handled automatically (computing the differential equations, obtaining the boundary conditions and solving the system) thus opening the door to more complicated problems with the presence of a larger number of topologies.

However, this automation comes at a price. In [68], indeed, the computation of a numerical grid for the B_{16} topology takes $\sim$ 12 hours. Even considering a factor 1.5/2 related to the bigger size of the system (56 equations for $\tilde{B}_{16}$ against 36 for B_{16}), we are a factor 10/15 slower with respect to the case of NC DY. This big difference in time is mainly due to the state of the system of differential equations. In the previous case, in fact, we have

[6] The error is estimated by considering the relative contribution of the last 3 terms in the series expansion over the complete series, both evaluated at half the radius of convergence.

JHEP07(2024)265

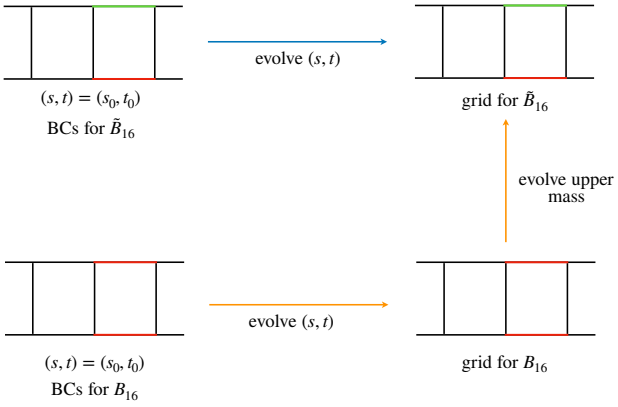

Figure 5. The two possibilities for creating a numerical grid for the $\tilde{B}_{16}$ topology. The first one, represented by the blue line, is to get the BCs for $\tilde{B}_{16}$ and then use the diff. eqs. w.r.t. s and t for obtaining the final grid. The second one, indicated by the orange lines, is to obtain the BCs for B_{16}, use the diff. eqs. for creating a grid in s and t for B_{16} and, finally, use it as new BCs for evolving B_{16} to $\tilde{B}_{16}$.

put a strong effort in simplifying the system by choosing a suitable change of basis to cast the system in pre-canonical form. This simpler form of the system enormously speeds up the computation. On the contrary, in this work, we have taken the MIs suggested by Kira and we have blindly written down their differential equations. This means that, other than standard algebraic simplifications, we have not performed any other optimization. Finding a change of basis which simplifies the system of differential equations is indeed important. However, it requires a big effort and a profound knowledge of the problem, while this blind approach relies only on computational power.

A second comment applies to the possibility of using AMFlow for the evaluation of the MIs in all the points of the phase-space. The evaluation of all the MIs takes $\sim$ 3h15m per point, running on 8 cores and asking for a precision of 16 digits. By using the same setup as the one used for SeaSyde, the complete run would approximately take 130 days.[7]

A final comment regards a severe limiting factor when working with numerical grids. Usually, all the input parameters are fixed to their numerical values and they cannot be modified without rerunning the final steps of the calculation. This requires a large amount of time. The series expansion approach, however, can be exploited for providing, with limited additional work, also the dependence on an additional variable e.g. $\delta M_W \equiv M_W - \bar{M}_W$, where $\bar{M}_W$ is a reference value for the mass of the W boson. This can be done following the idea of the mass evolution introduced in section 3.3.1. In particular, for each topology, we use the grid in (s,t), that we already have with a reference value $\bar{M}_W$, as a boundary condition, and we solve the differential equations w.r.t. M_W around $\bar{M}_W$. By doing so, it is possible to provide a grid in (s,t) where each point is a series in δM_W. Moreover, since the δM_W we are interested in are of the order of 0.1 GeV at most, only a small number of terms in the series is needed. Therefore, the solution can be computed in a small amount of time. For illustration, the evaluation of the δM_W dependence for the $\tilde{B}_{16}$ topology, for all

[7]The run-times have been estimated by using the latest public versions of each code.

JHEP07(2024)265

3250 points, has taken ~ 1.5 days, keeping 15 terms in the series. The difference between the SeaSyde solution, evaluated in $\delta M_W = 0.1\,\text{GeV}$, and AMFlow is on the 13th significant digit. This approach opens the possibility for implementing this kind of corrections in frontier studies like, but not limited to, the W-boson mass determination.

4 Infrared singularities and universal pole structure

The bare result presented in eq. (3.4), thanks to the renormalisation procedure described in section 2.2, is free of divergences of UV origin. Nevertheless, it still contains divergences of IR origin, generated by the exchange of soft and/or collinear massless partons. While these singularities are guaranteed to cancel in the computation of an IR-safe observable, where the two-loop amplitude is combined with the corresponding real emission contributions, they are expected to appear at intermediate stages of a calculation. Their presence requires the development of techniques to systematically handle and subtract them in a consistent way among the different contributions to an IR-safe observable.

At NLO, the Catani-Seymour dipole subtraction [98–100] and FKS subtraction [101] are the two methods most widely used. In their complete generality, they can be applied to any process and they have been implemented in automatic routines in several computational frameworks. At NNLO several techniques have been proposed (see e.g. [102] and references therein) but none of them can yet claim full generality. Regardless of the subtraction procedure, the IR poles are removed from the virtual contribution by using a process-independent subtraction operator. Such operators can in principle be different for each subtraction method but, because of the universal nature of the IR structure of the amplitude [103–111], they can at most differ from each other by a finite contribution.

In this paper, we present as our final result the amplitudes after the subtraction of the IR divergences according to the q_T subtraction formalism [79, 112]. We show them in the form of the hard function $H^{(1,1)}$, defined as the ratio of the 2-loop subtracted matrix element and the Born squared matrix element:

$$H^{(1,1)} = \frac{1}{16}\left[2\,\text{Re}\left(\frac{\langle\mathcal{M}^{(0)}|\mathcal{M}^{(1,1),fin}\rangle}{\langle\mathcal{M}^{(0)}|\mathcal{M}^{(0)}\rangle}\right)\right]. \tag{4.1}$$

The computation of the IR-subtracted matrix element $\langle\mathcal{M}^{(0)}|\mathcal{M}^{(1,1),fin}\rangle$ requires the knowledge of the subtracted two-loop amplitude $|\mathcal{M}^{(1,1),fin}\rangle$. We define it as follows:

$$|\mathcal{M}^{(1,1),fin}\rangle = |\mathcal{M}^{(1,1)}\rangle - \mathcal{I}^{(1,1)}|\mathcal{M}^{(0)}\rangle - \tilde{\mathcal{I}}^{(0,1)}|\mathcal{M}^{(1,0),fin}\rangle - \tilde{\mathcal{I}}^{(1,0)}|\mathcal{M}^{(0,1),fin}\rangle\,, \tag{4.2}$$

where the $\mathcal{I}$s are the IR subtraction operators and $|\mathcal{M}^{(1,0),fin}\rangle$, $|\mathcal{M}^{(0,1),fin}\rangle$ are the finite reminders of the one-loop QCD and EW amplitudes respectively:

$$|\mathcal{M}^{(1,0),fin}\rangle = |\mathcal{M}^{(1,0)}\rangle - \mathcal{I}^{(1,0)}|\mathcal{M}^{(0)}\rangle\,, \tag{4.3}$$

$$|\mathcal{M}^{(0,1),fin}\rangle = |\mathcal{M}^{(0,1)}\rangle - \mathcal{I}^{(0,1)}|\mathcal{M}^{(0)}\rangle\,. \tag{4.4}$$

The subtraction operators can be obtained from the ones used in the case of the NC DY process after appropriately changing the charges of the initial state quarks and after

JHEP07(2024)265

neglecting the contribution stemming from the exchange of a photon between two final state particles, which is not present in the case of CC DY. By indicating with Q_i the value of the electric charge of the particle i in positron units,[8] and with $C_F = \frac{N^2-1}{2N}$ the Casimir of the fundamental representation of SU(N), the subtraction operators at one loop read:

$$\mathcal{I}^{(1,0)} = \left(\frac{s}{\mu^2}\right)^{-\epsilon} C_F \left(-\frac{2}{\epsilon^2} - \frac{1}{\epsilon}(3+2i\pi) + \zeta_2\right), \tag{4.5}$$

$$\mathcal{I}^{(0,1)} = \left(\frac{s}{\mu^2}\right)^{-\epsilon} \left[\frac{Q_u^2+Q_d^2}{2}\left(-\frac{2}{\epsilon^2} - \frac{1}{\epsilon}(3+2i\pi) + \zeta_2\right) + \frac{4}{\epsilon}\Gamma_l^{(0,1)}\right], \tag{4.6}$$

where

$$\Gamma_l^{(0,1)} = -\frac{1}{4}\Big[Q_l^2\,(1-i\pi) + Q_l^2 \log\left(\frac{m_l^2}{s}\right) + \\ + 2Q_uQ_l \log\left(\frac{(2p_1\cdot p_4)}{s}\right) - 2Q_dQ_l \log\left(\frac{(2p_2\cdot p_4)}{s}\right)\Big]. \tag{4.7}$$

The two-loop subtraction operator for the mixed contribution reads:

$$\mathcal{I}^{(1,1)} = \left(\frac{s}{\mu^2}\right)^{-2\epsilon} C_F \Big[\frac{Q_u^2+Q_d^2}{2}\Big(\frac{4}{\epsilon^4} + \frac{1}{\epsilon^3}(12+8i\pi) + \frac{1}{\epsilon^2}(9-28\zeta_2+12i\pi) + \\ + \frac{1}{\epsilon}\left(-\frac{3}{2} + 6\zeta_2 - 24\zeta_3 - 4i\pi\zeta_2\right)\Big) + \left(-\frac{2}{\epsilon^2} - \frac{1}{\epsilon}(3+2i\pi) + \zeta_2\right)\frac{4}{\epsilon}\,\Gamma_l^{(0,1)}\Big]. \tag{4.8}$$

Following the same convention used in the case of the NC DY process, in eq. (4.2) the subtraction of the one-loop-like divergences from the two loop amplitude is performed by using the subtraction operators $\tilde{\mathcal{I}}^{(1,0)}$ and $\tilde{\mathcal{I}}^{(0,1)}$, which can be obtained from $\mathcal{I}^{(1,0)}$ and $\mathcal{I}^{(0,1)}$ by dropping the term proportional to ζ_2.

The approximation of the amplitude in the small lepton mass limit retains all the terms enhanced by $\log(m_l)$, divergent in the $m_\ell \to 0$ limit. The structure of these corrections reflects the universality property of the final-state collinear divergences, and is given, normalised to the Born squared matrix element, by

$$\lim_{m_\ell\to 0} \frac{\langle \mathcal{M}^{(0)}|\mathcal{M}^{(1,1),fin}\rangle}{\langle \mathcal{M}^{(0)}|\mathcal{M}^{(0)}\rangle} = K \;+\; \frac{C_F}{2}Q_l^2(-8+7\zeta_2-3i\pi)\Big[-\log\left(\frac{m_\ell^2}{s}\right) + \log^2\left(\frac{m_\ell^2}{s}\right)\Big], \tag{4.9}$$

where K represents all the other terms in the interference, constant in the $m_\ell \to 0$ limit. Note that the coefficients of the lepton mass logarithms are exactly with a factor half of those of the NC DY, indicating the universal behaviour of these logarithms.

5 Results

5.1 Numerical results

The evaluation of the finite IR-subtracted UV-renormalised hard function $H^{(1,1)}$, defined in eq. (4.1), requires the combination of several contributions, with a non-negligible evaluation time for the MIs. For this reason it is of practical interest to prepare a numerical grid,

[8] E.g. $Q_u = \frac{2}{3}$.

JHEP07(2024)265

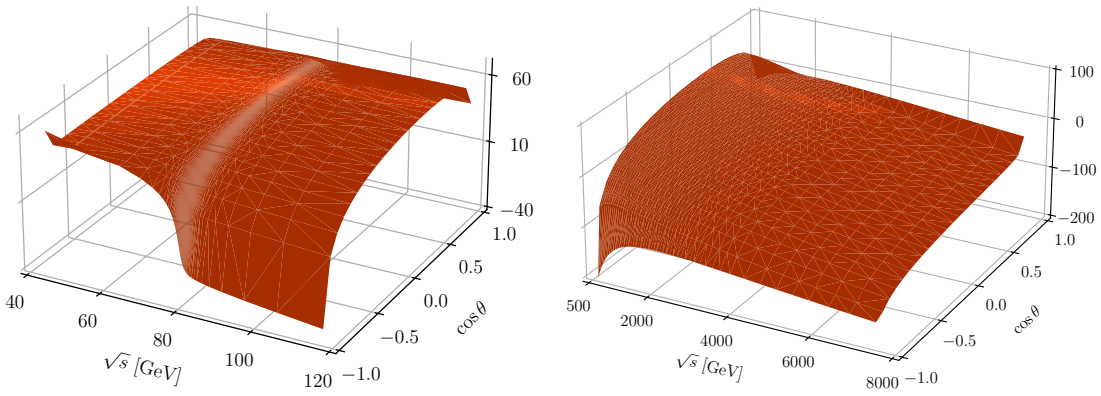

Figure 6. The complete correction to the finite hard function in the G_μ-scheme, due to $\mathcal{O}(\alpha\alpha_s)$ correction, in two different phase-space regions, as a function of $\sqrt{s}$ and $\cos\theta$. The correction is normalized by the Born and expressed in units $\frac{\alpha}{\pi}\frac{\alpha_s}{\pi}$.

which covers the whole phase space relevant in the applications at hadron colliders, making negligible the evaluation time of the results, at any arbitrary point. We consider the partonic centre-of-mass energy $\sqrt{s}$ and scattering angle $\cos\theta$ and compute a grid with respectively (130x25) points, covering the intervals $\sqrt{s} \in [40, 8000]$ GeV and $\cos\theta \in [-1, 1]$. The sampling is based on the known behaviour of the CC-DY NLO-EW distribution, with special care for the W resonance region, where a finer binning is necessary. We have verified that the interpolation describes the exact results with an accuracy, in the whole phase space, at least at the 10^{-3} level, guaranteed by the smoothness of the IR-subtracted $H^{(1,1)}$ function.

We present in figure 6 the hard function $H^{(1,1)}$ in the G_μ-scheme, which is normalised to the Born cross section and expressed, as a function of $\sqrt{s}$ and $\cos\theta$, in units $\frac{\alpha}{\pi}\frac{\alpha_s}{\pi}$. We consider for the partonic center-of-mass energy, two different intervals, namely $40 \leq \sqrt{s} \leq 120\,\text{GeV}$ and $500 \leq \sqrt{s} \leq 7500\,\text{GeV}$, while the range in $\cos\theta$ is $[-1, 1]$. In figure 6, we use the following parameters:

M_Z	91.1535 GeV	Γ_Z	2.4943 GeV
M_W	80.358 GeV	Γ_W	2.084 GeV
m_H	125.25 GeV	m_t	173.2 GeV

The possibility to have an exact dependence on the W-boson mass, within this numerical approach, is discussed in section 5.3.

We provide in table 1 a few benchmark values of the function $H^{(1,1)}$ in the G_μ-scheme, for different $\sqrt{s}$ and $\cos\theta$ choices.

5.2 Checks

The scattering amplitude develops UV and IR divergences, which appear as poles in the dimensional regularisation parameter ε. Their cancellation provides a non trivial check of the consistency of the calculation. This check exploits the restoration of some QED-like Ward identities, valid in the BFG. In the construction of the UV-finite renormalised propagator we observe the cancellation of the W self-energy wave function divergence against the one of the charge counterterms. We verify that the sum of external wave function factors, vertex and

JHEP07(2024)265

$\sqrt{s}$ [GeV]	$\cos\theta$	$H^{(1,1)}$
88.066	0	61.318
88.066	-0.66	45.970
222.362	0	48.189
222.362	-0.66	-15.753
1035.37	0	29.029
1035.37	-0.66	-6.990

Table 1. Benchmark values for the finite hard function, in the G_μ-scheme, due to $\mathcal{O}(\alpha\alpha_s)$ correction. The correction is normalized by the Born and expressed in units $\frac{\alpha}{\pi}\frac{\alpha_s}{\pi}$.

box corrections is UV finite, thanks to the validity of the above mentioned Ward identities, featuring only IR singularities. The latter have indeed a universal structure, leading to the independent construction of an IR subtraction term, presented in section 4. The singularities of this subtraction term exactly match those of the sum of wave function, vertex and box corrections, leaving a finite remainder, free of any divergence.

In several stages of our computations and checks, we have used GiNaC [113], HarmonicSums [114, 115], PolyLogTools [116] and LoopTools [117].

5.3 Full dependence on the W-boson mass in the numerical grids

In sections 3.3 and 3.4 we have introduced the idea of using the series expansion approach in order to provide a grid in (s,t) in which each point is a series expansion in δM_W, thus featuring the exact μ_W dependence. In this section we discuss the sensitivity to a parameter like the W-boson mass and the accuracy of a series expansion approach compared to the exact evaluation.

As an example, we consider the integral $\tilde{B}_{14}[1,1,1,1,0,1,1,0,1]$, which is defined as:

$$\int \frac{d^dk_1}{(2\pi)^d}\frac{d^dk_2}{(2\pi)^d}\frac{1}{\mathcal{D}_1\,(\mathcal{D}_2-\mu_W^2)\,\mathcal{D}_{12}\,\mathcal{D}_{1;1}\,\mathcal{D}^0_{2;1}\,\mathcal{D}_{1;12}\,\mathcal{D}_{2;12}\,\mathcal{D}^0_{1;3}\,(\mathcal{D}_{2;3}-m_\ell^2)} \tag{5.1}$$

with the $\mathcal{D}$s introduced in eq. (3.2). This integral can be represented graphically as

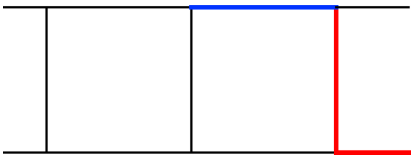

where the blue (red) indicates that a particle with mass μ_W (m_ℓ) is running in the line, and it appears, for example, in diagrams with the exchange of a photon and a W boson. In the left panel of figure 7 we plot the real and imaginary part of the integral, for different values of μ_W, as a function of $\sqrt{s}$, with $\cos\theta = 0.165$. The intensity of the color corresponds to different choices of δM_W, from $-500\,\text{MeV}$ to $500\,\text{MeV}$, in steps of $250\,\text{MeV}$. The shift of the peak position illustrates the sensitivity of this integral to the choice of the mass value. In the right panel of figure 7 we compare the exact evaluation of the integral[9] against different

[9]The exact solution is obtained using AMFlow, asking for a precision of 30 digits.

JHEP07(2024)265

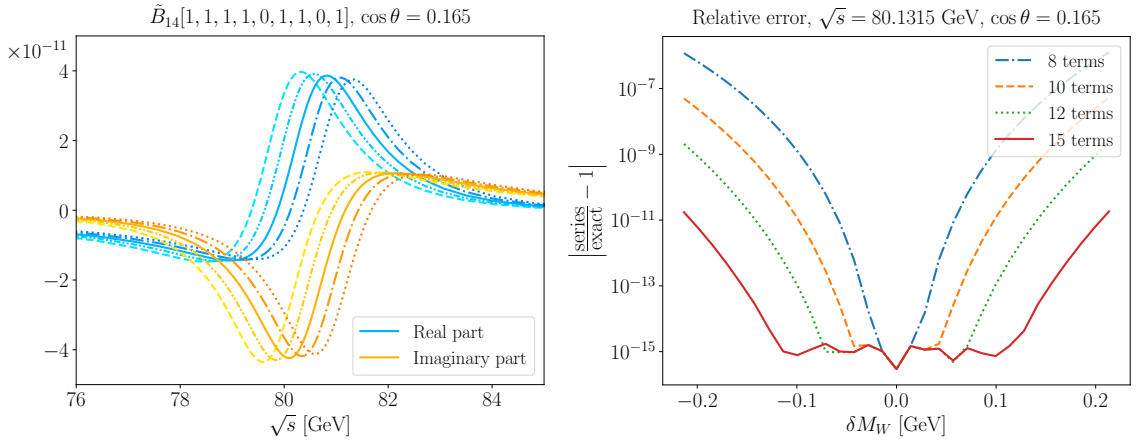

Figure 7. On the left panel we plot the real and imaginary part of the $\mathcal{O}(\varepsilon^0)$ of $\tilde{B}_{14}[1,1,1,1,0,1,1,0,1]$ for different values of δM_W. On the right panel we plot the relative error of the solution for different number of terms in the δM_W-series expansion, as a function of δM_W.

approximations. We consider $\sqrt{s} = 80.1315\,\text{GeV}$ in order to have a strong dependence on μ_W and $\cos\theta = 0.165$. The curves correspond to a different number of terms in the δM_W expansion, and their ratio with the exact result is plotted as a function of δM_W. From the plot we can see that if we consider only shifts in δM_W of order 100 MeV, 15 terms in the expansions are sufficient for maintaining a relative precision of 10^{-15}.

6 Conclusions

We have presented in this paper the details of the complete calculation, for the CC DY process, of its exact $\mathcal{O}(\alpha\alpha_s)$ two-loop virtual corrections. These results represent the companion to the ones discussed in ref. [68] for the NC DY case, with a higher level of technical complexity in the Master Integrals, because of the presence of two different mass values in the internal lines. When included in the MATRIX framework, for the evaluation of the fiducial cross sections, these results will allow a consistent simultaneous analysis of both NC and CC DY processes at NNLO QCD-EW level. Such consistency is required by the interplay between the two final states: for example, in the W-boson mass studies the NC DY channel plays a crucial calibration role, which would be spoiled if corrections at different orders were considered; at large lepton-pair transverse/invariant masses, CC and NC channels have different sensitivity to the parton-parton luminosities, thus allowing an effective reduction of the associated uncertainties, crucial in the New Physics searches.

The results have been obtained thanks to an increased level of automation of every step of the calculation, opening the way to the systematic study of the mixed QCD-EW corrections in other $2 \to 2$ scattering processes. In particular, it is worth mentioning the possibility to study in a uniform way all the relevant MIs, with 0,1, or 2 internal massive lines, in the same semi-analytical framework offered by the SEASYDE code, with excellent control on the cancellation of UV and IR divergences.

The flexibility of the differential equations technique to solve the MIs has been exploited to preserve the exact dependence on the W-boson mass, even when we prepare the numerical

JHEP07(2024)265

grid for the total correction factor. We achieve in this way excellent performances in the numerical evaluation together with full control on the accuracy of the result.

Acknowledgments

We would like to thank L. Buonocore, M. Grazzini, S. Kallweit, C. Savoini and F. Tramontano, for several interesting discussions during the development of the complete calculation of the NNLO QCD-EW corrections to NC DY and for a careful reading of the manuscript. T.A. is a Research Fellow of the Fonds de la Recherche Scientifique — FNRS. The work of S.D. has been partially funded by the European Union (ERC, MultiScaleAmp, Grant Agreement No. 101078449). Views and opinions expressed are however those of the author(s) only and do not necessarily reflect those of the European Union or the European Research Council Executive Agency. Neither the European Union nor the granting authority can be held responsible for them.

A Description of the supplementary material

In this appendix we describe the ancillary MATHEMATICA file CCDY_M11.m. This file contains the expression for $\langle\hat{\mathcal{M}}^{(0)}|\hat{\mathcal{M}}^{(1,1)}\rangle$ i.e. the unrenormalised interference term between the Born and the bare 2-loop amplitude as defined in eq. (3.4). In particular, within $|\hat{\mathcal{M}}^{(1,1)}\rangle$, there are all the pure 2-loop contribution, which are schematically depicted in figure 1-(a), (c), (f) and 2-(a), (c).

The result is provided as a sum of rational coefficients times a MI:

$$\sum_k c_k(s,t,\{m_i\},d)\; I_k(s,t,\{m_i\},d). \tag{A.1}$$

In the file, we make use of the following symbols:

$$\begin{aligned}
&\mathsf{mz} = \mu_Z\,, \quad \mathsf{mzC} = \mu_Z^*\,, \quad \mathsf{mw} = \mu_W\,, \quad \mathsf{mwC} = \mu_W^*\,,\\
&\mathsf{sw} = s_W\,, \quad \mathsf{swC} = s_W^*\,, \quad \mathsf{cw} = c_W\,, \quad \mathsf{cwC} = c_W^*\,,\\
&\mathsf{mm} = m_\ell\,, \quad \mathsf{mt} = m_t\,, \quad \mathsf{mh} = m_H\,, \quad \mathsf{d} = 4-2\varepsilon\\
&\mathsf{prefactor} = \left(\frac{\alpha}{4\pi}\right)^2 (4\pi)^8 \mu^{8-2d},
\end{aligned} \tag{A.2}$$

where s_W and c_W are the sine and cosine of the Weinberg angle, the * indicates the complex conjugate and μ is the renormalisation scale.

In the file, we label each MI as:

$$\mathsf{Topology}[\{\mathsf{masses\_\_\_}\},\mathsf{x\_\_\_}], \tag{A.3}$$

where Topology is the name of the topology, {masses___} is a list of the masses in the same order as they appear in the topology definition and x___ is the list of powers to which each denominator is raised. Additionally, all the integrals have a normalization factor $1/(2\pi)^d$ for each loop.

JHEP07(2024)265

For example, B16tilde[{mw, mz}, 0, 1, 1, 0, 0, 1, 1, 0, 0] is a short notation for:

$$\int \frac{d^d k_1}{(2\pi)^d} \frac{d^d k_2}{(2\pi)^d} \frac{1}{(\mathcal{D}_2 - \mu_W^2)\mathcal{D}_{12}\mathcal{D}_{1;12}(\mathcal{D}_{2;12} - \mu_Z^2)}. \tag{A.4}$$

We provide also the file integralfamilies.yaml with all the integral families expressed in a format suitable for a reduction with Kira.

References

[1] S.D. Drell and T.-M. Yan, *Massive Lepton Pair Production in Hadron-Hadron Collisions at High-Energies*, *Phys. Rev. Lett.* **25** (1970) 316 [*Erratum ibid.* **25** (1970) 902] [INSPIRE].

[2] CDF and D0 collaborations, *2012 Update of the Combination of CDF and D0 Results for the Mass of the W Boson*, arXiv:1204.0042 [INSPIRE].

[3] ATLAS collaboration, *Measurement of the W-boson mass in pp collisions at $\sqrt{s} = 7$ TeV with the ATLAS detector*, *Eur. Phys. J. C* **78** (2018) 110 [*Erratum ibid.* **78** (2018) 898] [arXiv:1701.07240] [INSPIRE].

[4] CDF and D0 collaborations, *Tevatron Run II combination of the effective leptonic electroweak mixing angle*, *Phys. Rev. D* **97** (2018) 112007 [arXiv:1801.06283] [INSPIRE].

[5] ATLAS collaboration, *Measurement of the effective leptonic weak mixing angle using electron and muon pairs from Z-boson decay in the ATLAS experiment at $\sqrt{s} = 8$ TeV*, ATLAS-CONF-2018-037, CERN, Geneva (2018).

[6] CMS collaboration, *Measurement of the Drell-Yan forward-backward asymmetry and of the effective leptonic weak mixing angle using proton-proton collisions at 13 TeV*, CMS-PAS-SMP-22-010, CERN, Geneva (2024).

[7] C.M. Carloni Calame et al., *Precision Measurement of the W-Boson Mass: Theoretical Contributions and Uncertainties*, *Phys. Rev. D* **96** (2017) 093005 [arXiv:1612.02841] [INSPIRE].

[8] E. Bagnaschi and A. Vicini, *Parton Density Uncertainties and the Determination of Electroweak Parameters at Hadron Colliders*, *Phys. Rev. Lett.* **126** (2021) 041801 [arXiv:1910.04726] [INSPIRE].

[9] A. Behring et al., *Estimating the impact of mixed QCD-electroweak corrections on the W-mass determination at the LHC*, *Phys. Rev. D* **103** (2021) 113002 [arXiv:2103.02671] [INSPIRE].

[10] L. Rottoli, P. Torrielli and A. Vicini, *Determination of the W-boson mass at hadron colliders*, *Eur. Phys. J. C* **83** (2023) 948 [arXiv:2301.04059] [INSPIRE].

[11] P. Torrielli, L. Rottoli and A. Vicini, *A new observable for W-mass determination*, *PoS* **RADCOR2023** (2024) 038 [arXiv:2308.15993] [INSPIRE].

[12] G. Altarelli, R.K. Ellis and G. Martinelli, *Large Perturbative Corrections to the Drell-Yan Process in QCD*, *Nucl. Phys. B* **157** (1979) 461 [INSPIRE].

[13] R. Hamberg, W.L. van Neerven and T. Matsuura, *A complete calculation of the order α_s^2 correction to the Drell-Yan K factor*, *Nucl. Phys. B* **359** (1991) 343 [INSPIRE].

JHEP07(2024)265

[14] R.V. Harlander and W.B. Kilgore, *Next-to-next-to-leading order Higgs production at hadron colliders*, *Phys. Rev. Lett.* **88** (2002) 201801 [hep-ph/0201206] [INSPIRE].

[15] C. Duhr, F. Dulat and B. Mistlberger, *Drell-Yan Cross Section to Third Order in the Strong Coupling Constant*, *Phys. Rev. Lett.* **125** (2020) 172001 [arXiv:2001.07717] [INSPIRE].

[16] C. Duhr, F. Dulat and B. Mistlberger, *Charged current Drell-Yan production at N^3LO*, *JHEP* **11** (2020) 143 [arXiv:2007.13313] [INSPIRE].

[17] C. Duhr and B. Mistlberger, *Lepton-pair production at hadron colliders at N^3LO in QCD*, *JHEP* **03** (2022) 116 [arXiv:2111.10379] [INSPIRE].

[18] C. Anastasiou, L.J. Dixon, K. Melnikov and F. Petriello, *Dilepton rapidity distribution in the Drell-Yan process at NNLO in QCD*, *Phys. Rev. Lett.* **91** (2003) 182002 [hep-ph/0306192] [INSPIRE].

[19] C. Anastasiou, L.J. Dixon, K. Melnikov and F. Petriello, *High precision QCD at hadron colliders: Electroweak gauge boson rapidity distributions at NNLO*, *Phys. Rev. D* **69** (2004) 094008 [hep-ph/0312266] [INSPIRE].

[20] K. Melnikov and F. Petriello, *Electroweak gauge boson production at hadron colliders through $\mathcal{O}(\alpha_s^2)$*, *Phys. Rev. D* **74** (2006) 114017 [hep-ph/0609070] [INSPIRE].

[21] S. Catani et al., *Vector boson production at hadron colliders: a fully exclusive QCD calculation at NNLO*, *Phys. Rev. Lett.* **103** (2009) 082001 [arXiv:0903.2120] [INSPIRE].

[22] S. Catani, G. Ferrera and M. Grazzini, *W Boson Production at Hadron Colliders: The Lepton Charge Asymmetry in NNLO QCD*, *JHEP* **05** (2010) 006 [arXiv:1002.3115] [INSPIRE].

[23] S. Camarda, L. Cieri and G. Ferrera, *Drell-Yan lepton-pair production: qT resummation at N3LL accuracy and fiducial cross sections at N3LO*, *Phys. Rev. D* **104** (2021) L111503 [arXiv:2103.04974] [INSPIRE].

[24] X. Chen et al., *Third-Order Fiducial Predictions for Drell-Yan Production at the LHC*, *Phys. Rev. Lett.* **128** (2022) 252001 [arXiv:2203.01565] [INSPIRE].

[25] T. Neumann and J. Campbell, *Fiducial Drell-Yan production at the LHC improved by transverse-momentum resummation at N4LLp+N3LO*, *Phys. Rev. D* **107** (2023) L011506 [arXiv:2207.07056] [INSPIRE].

[26] J. Campbell and T. Neumann, *Third order QCD predictions for fiducial W-boson production*, *JHEP* **11** (2023) 127 [arXiv:2308.15382] [INSPIRE].

[27] X. Chen et al., *Dilepton Rapidity Distribution in Drell-Yan Production to Third Order in QCD*, *Phys. Rev. Lett.* **128** (2022) 052001 [arXiv:2107.09085] [INSPIRE].

[28] X. Chen et al., *Transverse mass distribution and charge asymmetry in W boson production to third order in QCD*, *Phys. Lett. B* **840** (2023) 137876 [arXiv:2205.11426] [INSPIRE].

[29] S. Moch and A. Vogt, *Higher-order soft corrections to lepton pair and Higgs boson production*, *Phys. Lett. B* **631** (2005) 48 [hep-ph/0508265] [INSPIRE].

[30] E. Laenen and L. Magnea, *Threshold resummation for electroweak annihilation from DIS data*, *Phys. Lett. B* **632** (2006) 270 [hep-ph/0508284] [INSPIRE].

[31] V. Ravindran, *On Sudakov and soft resummations in QCD*, *Nucl. Phys. B* **746** (2006) 58 [hep-ph/0512249] [INSPIRE].

[32] V. Ravindran, *Higher-order threshold effects to inclusive processes in QCD*, *Nucl. Phys. B* **752** (2006) 173 [hep-ph/0603041] [INSPIRE].

JHEP07(2024)265

[33] D. de Florian and J. Mazzitelli, *A next-to-next-to-leading order calculation of soft-virtual cross sections*, *JHEP* **12** (2012) 088 [arXiv:1209.0673] [INSPIRE].

[34] T. Ahmed, M. Mahakhud, N. Rana and V. Ravindran, *Drell-Yan Production at Threshold to Third Order in QCD*, *Phys. Rev. Lett.* **113** (2014) 112002 [arXiv:1404.0366] [INSPIRE].

[35] S. Catani et al., *Threshold resummation at N^3LL accuracy and soft-virtual cross sections at N^3LO*, *Nucl. Phys. B* **888** (2014) 75 [arXiv:1405.4827] [INSPIRE].

[36] Y. Li, A. von Manteuffel, R.M. Schabinger and H.X. Zhu, *Soft-virtual corrections to Higgs production at N^3LO*, *Phys. Rev. D* **91** (2015) 036008 [arXiv:1412.2771] [INSPIRE].

[37] A. A H, P. Mukherjee and V. Ravindran, *Next to soft corrections to Drell-Yan and Higgs boson productions*, *Phys. Rev. D* **105** (2022) 094035 [arXiv:2006.06726] [INSPIRE].

[38] S. Dittmaier and M. Krämer, *Electroweak radiative corrections to W boson production at hadron colliders*, *Phys. Rev. D* **65** (2002) 073007 [hep-ph/0109062] [INSPIRE].

[39] U. Baur and D. Wackeroth, *Electroweak radiative corrections to $p\bar{p} \to W^{\pm} \to \ell^{\pm}\nu$ beyond the pole approximation*, *Phys. Rev. D* **70** (2004) 073015 [hep-ph/0405191] [INSPIRE].

[40] V.A. Zykunov, *Radiative corrections to the Drell-Yan process at large dilepton invariant masses*, *Phys. Atom. Nucl.* **69** (2006) 1522 [INSPIRE].

[41] A. Arbuzov et al., *One-loop corrections to the Drell-Yan process in SANC. I. The charged current case*, *Eur. Phys. J. C* **46** (2006) 407 [*Erratum ibid.* **50** (2007) 505] [hep-ph/0506110] [INSPIRE].

[42] C.M. Carloni Calame, G. Montagna, O. Nicrosini and A. Vicini, *Precision electroweak calculation of the charged current Drell-Yan process*, *JHEP* **12** (2006) 016 [hep-ph/0609170] [INSPIRE].

[43] U. Baur et al., *Electroweak radiative corrections to neutral current Drell-Yan processes at hadron colliders*, *Phys. Rev. D* **65** (2002) 033007 [hep-ph/0108274] [INSPIRE].

[44] V.A. Zykunov, *Weak radiative corrections to Drell-Yan process for large invariant mass of di-lepton pair*, *Phys. Rev. D* **75** (2007) 073019 [hep-ph/0509315] [INSPIRE].

[45] C.M. Carloni Calame, G. Montagna, O. Nicrosini and A. Vicini, *Precision electroweak calculation of the production of a high transverse-momentum lepton pair at hadron colliders*, *JHEP* **10** (2007) 109 [arXiv:0710.1722] [INSPIRE].

[46] A. Arbuzov et al., *One-loop corrections to the Drell-Yan process in SANC. (II). The neutral current case*, *Eur. Phys. J. C* **54** (2008) 451 [arXiv:0711.0625] [INSPIRE].

[47] S. Dittmaier and M. Huber, *Radiative corrections to the neutral-current Drell-Yan process in the Standard Model and its minimal supersymmetric extension*, *JHEP* **01** (2010) 060 [arXiv:0911.2329] [INSPIRE].

[48] C. Bernaciak and D. Wackeroth, *Combining NLO QCD and Electroweak Radiative Corrections to W boson Production at Hadron Colliders in the POWHEG Framework*, *Phys. Rev. D* **85** (2012) 093003 [arXiv:1201.4804] [INSPIRE].

[49] L. Barze et al., *Implementation of electroweak corrections in the POWHEG BOX: single W production*, *JHEP* **04** (2012) 037 [arXiv:1202.0465] [INSPIRE].

[50] L. Barze et al., *Neutral current Drell-Yan with combined QCD and electroweak corrections in the POWHEG BOX*, *Eur. Phys. J. C* **73** (2013) 2474 [arXiv:1302.4606] [INSPIRE].

[51] R. Frederix et al., *The automation of next-to-leading order electroweak calculations*, *JHEP* **11** (2018) 085 [*Erratum ibid.* **11** (2021) 085] [arXiv:1804.10017] [INSPIRE].

JHEP07(2024)265

[52] M. Chiesa, C.L. Del Pio and F. Piccinini, *On electroweak corrections to neutral current Drell-Yan with the POWHEG BOX*, *Eur. Phys. J. C* **84** (2024) 539 [arXiv:2402.14659] [INSPIRE].

[53] D. de Florian, M. Der and I. Fabre, *QCD⊕QED NNLO corrections to Drell Yan production*, *Phys. Rev. D* **98** (2018) 094008 [arXiv:1805.12214] [INSPIRE].

[54] M. Delto, M. Jaquier, K. Melnikov and R. Röntsch, *Mixed QCD⊗QED corrections to on-shell Z boson production at the LHC*, *JHEP* **01** (2020) 043 [arXiv:1909.08428] [INSPIRE].

[55] L. Cieri, D. de Florian, M. Der and J. Mazzitelli, *Mixed QCD⊗QED corrections to exclusive Drell Yan production using the q_T -subtraction method*, *JHEP* **09** (2020) 155 [arXiv:2005.01315] [INSPIRE].

[56] R. Bonciani, F. Buccioni, R. Mondini and A. Vicini, *Double-real corrections at $\mathcal{O}(\alpha\alpha_s)$ to single gauge boson production*, *Eur. Phys. J. C* **77** (2017) 187 [arXiv:1611.00645] [INSPIRE].

[57] R. Bonciani et al., *NNLO QCD×EW corrections to Z production in the $q\bar{q}$ channel*, *Phys. Rev. D* **101** (2020) 031301 [arXiv:1911.06200] [INSPIRE].

[58] R. Bonciani, F. Buccioni, N. Rana and A. Vicini, *Next-to-Next-to-Leading Order Mixed QCD-Electroweak Corrections to on-Shell Z Production*, *Phys. Rev. Lett.* **125** (2020) 232004 [arXiv:2007.06518] [INSPIRE].

[59] R. Bonciani, F. Buccioni, N. Rana and A. Vicini, *On-shell Z boson production at hadron colliders through $\mathcal{O}(\alpha\alpha_s)$*, *JHEP* **02** (2022) 095 [arXiv:2111.12694] [INSPIRE].

[60] F. Buccioni et al., *Mixed QCD-electroweak corrections to on-shell Z production at the LHC*, *Phys. Lett. B* **811** (2020) 135969 [arXiv:2005.10221] [INSPIRE].

[61] A. Behring et al., *Mixed QCD-electroweak corrections to W-boson production in hadron collisions*, *Phys. Rev. D* **103** (2021) 013008 [arXiv:2009.10386] [INSPIRE].

[62] S. Dittmaier, A. Huss and C. Schwinn, *Mixed QCD-electroweak $\mathcal{O}(\alpha_s\alpha)$ corrections to Drell-Yan processes in the resonance region: pole approximation and non-factorizable corrections*, *Nucl. Phys. B* **885** (2014) 318 [arXiv:1403.3216] [INSPIRE].

[63] S. Dittmaier, A. Huss and C. Schwinn, *Dominant mixed QCD-electroweak $O(\alpha_s\alpha)$ corrections to Drell-Yan processes in the resonance region*, *Nucl. Phys. B* **904** (2016) 216 [arXiv:1511.08016] [INSPIRE].

[64] S. Dittmaier, T. Schmidt and J. Schwarz, *Mixed NNLO QCD × electroweak corrections of $\mathcal{O}(N_f\alpha_s\alpha)$ to single-W/Z production at the LHC*, *JHEP* **12** (2020) 201 [arXiv:2009.02229] [INSPIRE].

[65] S. Dittmaier, A. Huss and J. Schwarz, *Mixed NNLO QCD × electroweak corrections to single-Z production in pole approximation: differential distributions and forward-backward asymmetry*, *JHEP* **05** (2024) 170 [arXiv:2401.15682] [INSPIRE].

[66] R. Bonciani et al., *Mixed Strong-Electroweak Corrections to the Drell-Yan Process*, *Phys. Rev. Lett.* **128** (2022) 012002 [arXiv:2106.11953] [INSPIRE].

[67] F. Buccioni et al., *Mixed QCD-electroweak corrections to dilepton production at the LHC in the high invariant mass region*, *JHEP* **06** (2022) 022 [arXiv:2203.11237] [INSPIRE].

[68] T. Armadillo et al., *Two-loop mixed QCD-EW corrections to neutral current Drell-Yan*, *JHEP* **05** (2022) 072 [arXiv:2201.01754] [INSPIRE].

JHEP07(2024)265

[69] R. Bonciani, S. Di Vita, P. Mastrolia and U. Schubert, *Two-Loop Master Integrals for the mixed EW-QCD virtual corrections to Drell-Yan scattering*, *JHEP* **09** (2016) 091 [arXiv:1604.08581] [INSPIRE].

[70] F. Moriello, *Generalised power series expansions for the elliptic planar families of Higgs + jet production at two loops*, *JHEP* **01** (2020) 150 [arXiv:1907.13234] [INSPIRE].

[71] M. Hidding, *DiffExp, a Mathematica package for computing Feynman integrals in terms of one-dimensional series expansions*, *Comput. Phys. Commun.* **269** (2021) 108125 [arXiv:2006.05510] [INSPIRE].

[72] T. Armadillo et al., *Evaluation of Feynman integrals with arbitrary complex masses via series expansions*, *Comput. Phys. Commun.* **282** (2023) 108545 [arXiv:2205.03345] [INSPIRE].

[73] L. Buonocore, S. Kallweit, L. Rottoli and M. Wiesemann, *Linear power corrections for two-body kinematics in the q_T subtraction formalism*, *Phys. Lett. B* **829** (2022) 137118 [arXiv:2111.13661] [INSPIRE].

[74] S. Camarda, L. Cieri and G. Ferrera, *Fiducial perturbative power corrections within the q_T subtraction formalism*, *Eur. Phys. J. C* **82** (2022) 575 [arXiv:2111.14509] [INSPIRE].

[75] M. Grazzini, S. Kallweit and M. Wiesemann, *Fully differential NNLO computations with MATRIX*, *Eur. Phys. J. C* **78** (2018) 537 [arXiv:1711.06631] [INSPIRE].

[76] M. Heller, A. von Manteuffel, R.M. Schabinger and H. Spiesberger, *Mixed EW-QCD two-loop amplitudes for $q\bar{q} \to \ell^+\ell^-$ and γ_5 scheme independence of multi-loop corrections*, *JHEP* **05** (2021) 213 [arXiv:2012.05918] [INSPIRE].

[77] M. Heller, A. von Manteuffel and R.M. Schabinger, *Multiple polylogarithms with algebraic arguments and the two-loop EW-QCD Drell-Yan master integrals*, *Phys. Rev. D* **102** (2020) 016025 [arXiv:1907.00491] [INSPIRE].

[78] S.M. Hasan and U. Schubert, *Master Integrals for the mixed QCD-QED corrections to the Drell-Yan production of a massive lepton pair*, *JHEP* **11** (2020) 107 [arXiv:2004.14908] [INSPIRE].

[79] L. Buonocore et al., *Mixed QCD-EW corrections to $pp \to \ell\nu_\ell + X$ at the LHC*, *Phys. Rev. D* **103** (2021) 114012 [arXiv:2102.12539] [INSPIRE].

[80] F.V. Tkachov, *A theorem on analytical calculability of 4-loop renormalization group functions*, *Phys. Lett. B* **100** (1981) 65 [INSPIRE].

[81] K.G. Chetyrkin and F.V. Tkachov, *Integration by parts: The algorithm to calculate β-functions in 4 loops*, *Nucl. Phys. B* **192** (1981) 159 [INSPIRE].

[82] T. Gehrmann and E. Remiddi, *Differential equations for two loop four point functions*, *Nucl. Phys. B* **580** (2000) 485 [hep-ph/9912329] [INSPIRE].

[83] G. Degrassi and A. Vicini, *Two loop renormalization of the electric charge in the standard model*, *Phys. Rev. D* **69** (2004) 073007 [hep-ph/0307122] [INSPIRE].

[84] A. Denner, S. Dittmaier, M. Roth and L.H. Wieders, *Electroweak corrections to charged-current $e^+e^- \to 4$ fermion processes: Technical details and further results*, *Nucl. Phys. B* **724** (2005) 247 [hep-ph/0505042] [INSPIRE].

[85] A. Denner and S. Dittmaier, *Electroweak Radiative Corrections for Collider Physics*, *Phys. Rept.* **864** (2020) 1 [arXiv:1912.06823] [INSPIRE].

[86] A. Sirlin, *Radiative Corrections in the $SU(2)_L \times U(1)$ Theory: A Simple Renormalization Framework*, *Phys. Rev. D* **22** (1980) 971 [INSPIRE].

JHEP07(2024)265

[87] B.A. Kniehl, *Two Loop Corrections to the Vacuum Polarizations in Perturbative QCD*, *Nucl. Phys. B* **347** (1990) 86 [INSPIRE].

[88] A. Djouadi and P. Gambino, *Electroweak gauge bosons selfenergies: Complete QCD corrections*, *Phys. Rev. D* **49** (1994) 3499 [*Erratum ibid.* **53** (1996) 4111] [hep-ph/9309298] [INSPIRE].

[89] A. Denner, G. Weiglein and S. Dittmaier, *Application of the background field method to the electroweak standard model*, *Nucl. Phys. B* **440** (1995) 95 [hep-ph/9410338] [INSPIRE].

[90] T. Hahn, *Generating Feynman diagrams and amplitudes with FeynArts 3*, *Comput. Phys. Commun.* **140** (2001) 418 [hep-ph/0012260] [INSPIRE].

[91] P. Nogueira, *Automatic Feynman Graph Generation*, *J. Comput. Phys.* **105** (1993) 279 [INSPIRE].

[92] J.A.M. Vermaseren, *New features of FORM*, math-ph/0010025 [INSPIRE].

[93] P. Maierhöfer, J. Usovitsch and P. Uwer, *Kira — A Feynman integral reduction program*, *Comput. Phys. Commun.* **230** (2018) 99 [arXiv:1705.05610] [INSPIRE].

[94] R.N. Lee, *LiteRed 1.4: a powerful tool for reduction of multiloop integrals*, *J. Phys. Conf. Ser.* **523** (2014) 012059 [arXiv:1310.1145] [INSPIRE].

[95] R.N. Lee, *Presenting LiteRed: a tool for the Loop InTEgrals REDuction*, arXiv:1212.2685 [INSPIRE].

[96] J. Frenkel and J.C. Taylor, *Exponentiation of Leading Infrared Divergences in Massless Yang-Mills Theories*, *Nucl. Phys. B* **116** (1976) 185 [INSPIRE].

[97] X. Liu and Y.-Q. Ma, *AMFlow: A Mathematica package for Feynman integrals computation via auxiliary mass flow*, *Comput. Phys. Commun.* **283** (2023) 108565 [arXiv:2201.11669] [INSPIRE].

[98] S. Catani and M.H. Seymour, *The dipole formalism for the calculation of QCD jet cross-sections at next-to-leading order*, *Phys. Lett. B* **378** (1996) 287 [hep-ph/9602277] [INSPIRE].

[99] S. Catani and M.H. Seymour, *A general algorithm for calculating jet cross-sections in NLO QCD*, *Nucl. Phys. B* **485** (1997) 291 [hep-ph/9605323] [INSPIRE].

[100] S. Catani, S. Dittmaier, M.H. Seymour and Z. Trocsanyi, *The dipole formalism for next-to-leading order QCD calculations with massive partons*, *Nucl. Phys. B* **627** (2002) 189 [hep-ph/0201036] [INSPIRE].

[101] S. Frixione, Z. Kunszt and A. Signer, *Three jet cross-sections to next-to-leading order*, *Nucl. Phys. B* **467** (1996) 399 [hep-ph/9512328] [INSPIRE].

[102] J.R. Andersen et al., *Les Houches 2017: Physics at TeV Colliders Standard Model Working Group Report*, arXiv:1803.07977 [INSPIRE].

[103] S. Catani, *The singular behavior of QCD amplitudes at two loop order*, *Phys. Lett. B* **427** (1998) 161 [hep-ph/9802439] [INSPIRE].

[104] G.F. Sterman and M.E. Tejeda-Yeomans, *Multiloop amplitudes and resummation*, *Phys. Lett. B* **552** (2003) 48 [hep-ph/0210130] [INSPIRE].

[105] T. Becher and M. Neubert, *Infrared singularities of scattering amplitudes in perturbative QCD*, *Phys. Rev. Lett.* **102** (2009) 162001 [*Erratum ibid.* **111** (2013) 199905] [arXiv:0901.0722] [INSPIRE].

[106] E. Gardi and L. Magnea, *Factorization constraints for soft anomalous dimensions in QCD scattering amplitudes*, *JHEP* **03** (2009) 079 [arXiv:0901.1091] [INSPIRE].

JHEP07(2024)265

[107] W.B. Kilgore and C. Sturm, *Two-Loop Virtual Corrections to Drell-Yan Production at order $\alpha_s\alpha^3$*, *Phys. Rev. D* **85** (2012) 033005 [arXiv:1107.4798] [INSPIRE].

[108] W.B. Kilgore, *The Two-Loop Infrared Structure of Amplitudes with Mixed Gauge Groups*, *Eur. Phys. J. C* **73** (2013) 2603 [arXiv:1308.1055] [INSPIRE].

[109] T. Becher and K. Melnikov, *Two-loop QED corrections to Bhabha scattering*, *JHEP* **06** (2007) 084 [arXiv:0704.3582] [INSPIRE].

[110] T. Ahmed, J.M. Henn and M. Steinhauser, *High energy behaviour of form factors*, *JHEP* **06** (2017) 125 [arXiv:1704.07846] [INSPIRE].

[111] J. Blümlein, P. Marquard and N. Rana, *Asymptotic behavior of the heavy quark form factors at higher order*, *Phys. Rev. D* **99** (2019) 016013 [arXiv:1810.08943] [INSPIRE].

[112] L. Buonocore, M. Grazzini and F. Tramontano, *The q_T subtraction method: electroweak corrections and power suppressed contributions*, *Eur. Phys. J. C* **80** (2020) 254 [arXiv:1911.10166] [INSPIRE].

[113] J. Vollinga and S. Weinzierl, *Numerical evaluation of multiple polylogarithms*, *Comput. Phys. Commun.* **167** (2005) 177 [hep-ph/0410259] [INSPIRE].

[114] J. Ablinger, *A Computer Algebra Toolbox for Harmonic Sums Related to Particle Physics*, M.Sc. thesis, Linz University, Austria (2009) [arXiv:1011.1176] [INSPIRE].

[115] J. Ablinger, *The package HarmonicSums: Computer Algebra and Analytic aspects of Nested Sums*, *PoS* **LL2014** (2014) 019 [arXiv:1407.6180] [INSPIRE].

[116] C. Duhr and F. Dulat, *PolyLogTools — polylogs for the masses*, *JHEP* **08** (2019) 135 [arXiv:1904.07279] [INSPIRE].

[117] T. Hahn and M. Perez-Victoria, *Automatized one loop calculations in four-dimensions and D-dimensions*, *Comput. Phys. Commun.* **118** (1999) 153 [hep-ph/9807565] [INSPIRE].

JHEP07(2024)265